

Southampton Preprint SHEP 95-18
 Edinburgh Preprint 95/551
 Marseille Preprint CPT-95/PE.3218
 hep-ph/9506398

Lattice Study of the Decay $\bar{B}^0 \rightarrow \rho^+ l^- \bar{\nu}_l$: Model-Independent Determination of $|V_{ub}|$

UKQCD Collaboration

J M Flynn, J Nieves

Department of Physics, University of Southampton, Southampton SO17 1BJ,
 UK

**K C Bowler, N M Hazel, D S Henty, H Hoerber¹, R D Kenway and
 D G Richards**

Department of Physics & Astronomy, The University of Edinburgh, Edinburgh
 EH9 3JZ, Scotland

B J Gough

Theoretical Physics MS106, Fermilab, Batavia IL 60510, USA

H P Shanahan

Department of Physics & Astronomy, University of Glasgow, Glasgow
 G12 8QQ, Scotland

L P Lellouch

Centre de Physique Theorique, CNRS Luminy, F-13288 Marseille Cedex 9,
 France²

Abstract

¹Present address: HLRZ, 52425 Jülich and DESY, Hamburg, Germany

²Unité Propre de Recherche 7061

We present results of a lattice computation of the vector and axial-vector current matrix elements relevant for the semileptonic decay $\bar{B}^0 \rightarrow \rho^+ l^- \bar{\nu}_l$. The computations are performed in the quenched approximation of lattice QCD on a $24^3 \times 48$ lattice at $\beta = 6.2$, using an $\mathcal{O}(a)$ improved fermionic action. Our principal result is for the differential decay rate, $d\Gamma/dq^2$, for the decay $\bar{B}^0 \rightarrow \rho^+ l^- \bar{\nu}_l$ in a region beyond the charm threshold, allowing a model-independent extraction of $|V_{ub}|$ from experimental measurements. Heavy quark symmetry relations between radiative and semileptonic decays of \bar{B} mesons into light vector mesons are also discussed.

1 Introduction

The experimental determination of the Cabibbo-Kobayashi-Maskawa (CKM) [1, 2] matrix elements is vital because they control the hadronic sector of the Standard Model, determining CP violation and flavour mixing. The magnitudes and phases of these matrix elements must be established to make the Standard Model predictive, to determine the angles and area of the unitarity triangle, and to look for any inconsistency between the Standard Model and the experimental data which would point to new physics.

The CKM element V_{ub} is one of the most poorly known, currently uncertain to within a factor of two or three (at 90% CL) in magnitude [3]. The determination of $|V_{ub}|$ has traditionally been made from inclusive $b \rightarrow u$ semileptonic decays [4], looking at the lepton energy spectrum beyond the endpoint for decays to charmed final states. These determinations rely on models incorporating nonperturbative QCD effects to relate the measured spectrum to theoretical predictions. Models used include the quark model [5] and bound-state models [6]–[8] together with attempts to combine features from both [9]. This results in the inclusion of an additional error reflecting the range of models used [10].

In this paper we propose a model-independent method to determine $|V_{ub}|$ from the exclusive semileptonic charmless B decay $\bar{B}^0 \rightarrow \rho^+ l^- \bar{\nu}_l$, which should be measured with improved accuracy in B factories and at e^+e^- and hadron colliders in the near future. Currently, only an upper bound exists [11] for the total decay rate, but new experimental results should be available soon [12].

We will show how lattice QCD calculations, which incorporate nonperturbative QCD effects in a systematic way, can be used to extract $|V_{ub}|$ from experimental measurements of $\bar{B}^0 \rightarrow \rho^+ l^- \bar{\nu}_l$. Exclusive B decays have already proved useful for extracting the value of $|V_{cb}|$ by studying the process $\bar{B} \rightarrow D^* l \bar{\nu}_l$ [13]–[19].

We have also analysed relations between the exclusive processes $\bar{B} \rightarrow K^* \gamma$ and $\bar{B}^0 \rightarrow \rho^+ l^- \bar{\nu}_l$ which follow from heavy quark symmetry (HQS) [20]. We discuss the utility of these relations for determining $|V_{ub}|$ from the experimental measurements of $B(\bar{B} \rightarrow K^* \gamma)$ and $B(b \rightarrow s \gamma)$ [21]–[24].

2 Form Factors

The matrix elements we will be considering are of the $V - A$ weak current between \bar{B} and ρ mesons and of the magnetic moment operator between \bar{B} and K^* mesons [25]. For $\bar{B}^0 \rightarrow \rho^+ l^- \bar{\nu}_l$ the matrix element is,

$$\langle \rho(k, \eta) | \bar{u} \gamma_\mu (1 - \gamma_5) b | \bar{B}(p) \rangle = \eta^{*\beta} T_{\mu\beta}, \quad (1)$$

with form factor decomposition,

$$T_{\mu\beta} = \frac{2V(q^2)}{m_B + m_\rho} \epsilon_{\mu\gamma\delta\beta} p^\gamma k^\delta - i(m_B + m_\rho) A_1(q^2) g_{\mu\beta}$$

$$+ i \frac{A_2(q^2)}{m_B + m_\rho} (p+k)_\mu q_\beta - i \frac{A(q^2)}{q^2} 2m_\rho q_\mu (p+k)_\beta, \quad (2)$$

where $q = p - k$ is the four-momentum transfer and η is the ρ polarisation vector. The form factor A can be written as

$$A(q^2) = A_0(q^2) - A_3(q^2), \quad (3)$$

where,

$$A_3(q^2) = \frac{m_B + m_\rho}{2m_\rho} A_1(q^2) - \frac{m_B - m_\rho}{2m_\rho} A_2(q^2), \quad (4)$$

with $A_0(0) = A_3(0)$. In the limit of zero lepton masses, the term proportional to A in equation (2) does not contribute to the total amplitude and hence to the decay rates. Pole dominance models suggest that V , A_i for $i = 1, 2, 3$ and A_0 correspond to 1^- , 1^+ and 0^- exchanges respectively in the t -channel [7].

The main contribution to the $\bar{B} \rightarrow K^* \gamma$ decay comes from the matrix element

$$\langle K^*(k, \eta) | \bar{s} \sigma_{\mu\nu} q^\nu b_R | \bar{B}(p) \rangle = \sum_{i=1}^3 C_\mu^i T_i(q^2), \quad (5)$$

where $q = p - k$ as above, η is now the K^* polarisation vector and

$$C_\mu^1 = 2\epsilon_{\mu\nu\lambda\rho} \eta^\nu p^\lambda k^\rho, \quad (6)$$

$$C_\mu^2 = \eta_\mu (m_B^2 - m_{K^*}^2) - \eta \cdot q (p+k)_\mu, \quad (7)$$

$$C_\mu^3 = \eta \cdot q \left(q_\mu - \frac{q^2}{m_B^2 - m_{K^*}^2} (p+k)_\mu \right). \quad (8)$$

For an on-shell photon with $q^2 = 0$, T_3 does not contribute to the $\bar{B} \rightarrow K^* \gamma$ amplitude and T_1 and T_2 are related by,

$$T_1(q^2=0) = iT_2(q^2=0). \quad (9)$$

Hence, for $\bar{B} \rightarrow K^* \gamma$, we need to determine T_1 and/or T_2 at the on-shell point.

Neglecting corrections suppressed by inverse powers of the heavy quark mass M , the following relations hold when q^2 is close to the maximum recoil value $q_{\max}^2 = (M - m_{\rho, K^*})^2$ [20]

$$V\Theta/\sqrt{M} = \text{const}, \quad A_1\Theta\sqrt{M} = \text{const}, \quad A_2\Theta/\sqrt{M} = \text{const}, \quad (10)$$

where Θ arises from the leading logarithmic corrections and is chosen to be 1 at the B mass [26],

$$\Theta = \Theta(M/m_B) = \left(\frac{\alpha_s(M)}{\alpha_s(m_B)} \right)^{\frac{2}{\beta_0}}. \quad (11)$$

In the calculations reported below, we will use $\beta_0 = 11$ in the quenched approximation and $\Lambda_{\text{QCD}} = 200 \text{ MeV}$. The matrix elements of the $V - A$ current and the magnetic moment operator between \bar{B} and identical³ light final-state vector mesons of mass m are related in the infinite heavy quark mass limit according to:

$$V(q^2) = 2T_1(q^2), \quad A_1(q^2) = 2iT_2(q^2), \quad (12)$$

for values of q^2 not too far from q_{max}^2 , or equivalently, for ω close to 1, where

$$\omega = v \cdot v' = \frac{M^2 + m^2 - q^2}{2Mm}. \quad (13)$$

Here, v and v' are the four-velocities of the heavy-light pseudoscalar meson and the light vector meson respectively.

The equations in (12) relate the physical decay processes $\bar{B}^0 \rightarrow \rho^+ l^- \bar{\nu}_l$ and $\bar{B}^- \rightarrow \rho^- \gamma$. If light flavour $SU(3)$ symmetry is respected then equation (12) relates the processes $\bar{B}^0 \rightarrow \rho^+ l^- \bar{\nu}_l$ and $\bar{B} \rightarrow K^* \gamma$ [20]. In the lattice calculations reported below we will test equation (12) directly for different values of the heavy quark mass using identical light meson states for both matrix elements.

In the literature, versions of equation (12) appear which rely on lowest order HQS but incorporate all $1/M$ corrections from kinematics [20, 21, 27]⁴. The modified relations become:

$$2T_1(q^2) = \frac{q^2 + M^2 - m^2}{2M} \frac{V(q^2)}{M + m} + \frac{M + m}{2M} A_1(q^2) \quad (14)$$

$$2iT_2(q^2) = \frac{[(M+m)^2 - q^2][(M-m)^2 - q^2]}{2M(M^2 - m^2)} \frac{V(q^2)}{M + m} + \frac{q^2 + M^2 - m^2}{2M} \frac{A_1(q^2)}{M - m} \quad (15)$$

3 Lattice Details

Lattice calculations with propagating quarks provide matrix elements for heavy quarks around the charm mass over a range of q^2 straddling $q^2 = 0$. In extracting form factors from these matrix elements, we can reach q_{max}^2 for A_1 and T_2 only, because the coefficients determining the contribution of the other form factors to the matrix elements of equations (1) and (5) vanish at this kinematic point. To obtain results relevant for B decays, we need to extrapolate in the heavy quark mass M to the b quark mass. This is simple for fixed ω , but, at the B scale, produces a range of q^2 values near q_{max}^2 and far from $q^2 = 0$.

³We assume isospin symmetry between the light u and d quarks.

⁴To incorporate properly the dynamical $1/M$ corrections it is necessary to consider operators of dimension four in the heavy quark expansion in addition to those of dimension three occurring at leading order.

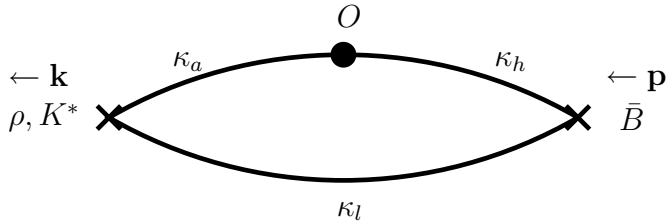


Figure 1 Labelling of quark hopping parameters for three-point correlator calculation.

The results described below come from 60 $SU(3)$ gauge configurations generated by the UKQCD collaboration on a $24^3 \times 48$ lattice at $\beta = 6.2$ in the quenched approximation. The $\mathcal{O}(a)$ improved Sheikholeslami–Wohlert (SW) [28] action was used for fermions, with “rotated” fermion fields appearing in all operators used for correlation function calculations [29]. The inverse lattice spacing determined from the ρ mass is $a^{-1} = 2.7(1)$ GeV [30]. Other physical quantities will lead to slightly different values for the lattice spacing ($a^{-1} = 2.7\text{--}3.0$ GeV [31]). The scale uncertainty should be reflected in the results for dimensional quantities.

Three-point correlators of the heavy-to-light two-fermion operators with a heavy pseudoscalar meson (the “ \bar{B} ” meson) and a light vector meson were calculated, as illustrated in figure 1. Matrix elements were extracted from these correlators by the method detailed in [32]–[35]. Four heavy-quark hopping parameters, $\kappa_h = 0.121, 0.125, 0.129, 0.133$, were used. For the propagator connecting the current operator to the light meson operator, two kappa values, $\kappa_a = 0.14144, 0.14226$, were available. The subscript a is for “active” to contrast this propagator with the “spectator” propagator joining the heavy-light meson to the light meson. These κ_a values straddle that for the strange quark, $0.1419(1)$ [30]. For $\kappa_h = 0.121, 0.129$, we used three light spectator hopping parameters, $\kappa_l = 0.14144, 0.14226, 0.14262$, and for $\kappa_h = 0.125, 0.133$ we used $\kappa_l = 0.14144$ only. The critical hopping parameter at this β is $\kappa_{\text{crit}} = 0.14315(1)$ [30].

The lattice calculations were performed with the heavy meson spatial momentum of magnitude 0 or 1, in lattice units of $\pi/12a$. The momentum injected at the operator insertion was varied to allow the modulus of the light meson spatial momentum to take values up to $\sqrt{2}$ in lattice units (although some of the momentum choices were too noisy to be used in fits). We refer to each combination of heavy and light meson three-momenta as a channel with the notation $|\mathbf{p}| \rightarrow |\mathbf{k}|$ in lattice units (for example $0 \rightarrow 1$ or $1 \rightarrow 1_\perp$ where the subscript \perp indicates that \mathbf{p} and \mathbf{k} are perpendicular).

The results below have been obtained using uncorrelated fits for the extrapolations in the heavy quark mass. The extraction of the form factors from the three-point correlation function data used correlated fits [32, 33]. Statistical errors are 68% confidence limits obtained from 250 bootstrap samples.

To make the best use of HQS, we pick momentum combinations which keep ω constant as the heavy-light meson mass varies. This allows us to scale in $1/M$ from the charm to the bottom mass scale and gives the form factors for the \bar{B} decays as functions of ω , and therefore as functions of q^2 . When the heavy-light meson is at rest, ω is independent of the heavy-light meson mass. As shown in reference [36] there are some additional channels, where the heavy-light meson is not at rest, but \mathbf{p} and \mathbf{k} are perpendicular, for which ω is very nearly constant as the heavy meson mass varies, and which can be used for heavy quark mass extrapolations. For those channels where ω is not strictly constant but which we nevertheless use in our study, the difference between the average ω value used in our analysis and that for each value of the heavy quark mass is always less than 3% [36].

For relating lattice results to the continuum, we have used the perturbative values for the renormalisation constants of the vector, axial and magnetic moment operators [37]:

$$Z_V = 0.83, \quad Z_A = 0.97, \quad Z_\sigma = 0.98. \quad (16)$$

The SW improved action reduces the leading discretisation errors from $\mathcal{O}(a)$ in the Wilson fermion action to $\mathcal{O}(\alpha_s a)$, but for quark masses m_Q around that of the charm quark, $\alpha_s m_Q a$ can be of order 10%. An estimate of the lattice artefacts can be obtained by comparing values of lattice renormalisation constants, computed from different matrix elements, in a non-perturbative way [38]. Numerical calculations have confirmed that errors of order 10% are present at our value of β in the matrix elements of vector and axial vector currents [15, 16]. We will therefore allow for an extra 10% systematic uncertainty in our results due to possible discretisation errors.

4 Semileptonic and Radiative Decays of Heavy-Light Mesons and Heavy Quark Symmetry

In this section we study the relations between the semileptonic and radiative decay processes of heavy-light mesons to light vector mesons. We will check the HQS relations of equation (12) and the size of $1/M$ corrections to these relations for different values of the heavy-light meson mass. For testing these relations we use our most accurate light-quark data, $\kappa_l = \kappa_a = 0.14144$: this ensures that the light degrees of freedom are the same for the semileptonic and radiative processes and allows us to check directly, without corrections due to $SU(3)$ symmetry breaking, the validity of HQS as M increases.

Specifically, we compare the form factors A_1 and V for the pseudoscalar to vector semileptonic decay,

$$P_{hl}(\kappa_h; \kappa_l = 0.14144) \rightarrow V_{ll}(\kappa_l = 0.14144)l\bar{\nu}_l, \quad (17)$$

with the form factors T_1 and T_2 for the pseudoscalar to vector radiative decay,

$$P_{hl}(\kappa_h; \kappa_l = 0.14144) \rightarrow V_{ll}(\kappa_l = 0.14144)\gamma, \quad (18)$$

for different values of the heavy quark mass, $\kappa_h = 0.121, 0.125, 0.129$ and 0.133 , and for different values of ω close to $\omega = 1$. The corresponding heavy-light pseudoscalar masses are in the range 1.6 GeV to 2.5 GeV. We have also extrapolated to the B scale and to the infinite heavy quark mass limit. We have used five momentum channels in our analysis⁵: $0 \rightarrow 0$, $0 \rightarrow 1$, $0 \rightarrow \sqrt{2}$, $1 \rightarrow 0$ and $1 \rightarrow 1_\perp$.

In all cases the ratios $V/2T_1$ and $A_1/2iT_2$ are consistent with unity in the heavy quark mass limit, as predicted by HQS, although for certain channels the ratio $V/2T_1$ departs from 1 by up to 75% at the charm scale. This constitutes a non-trivial test of HQS predictions. These results are illustrated in figures 2 and 3.

In figure 2 we show the ratios $V/2T_1$ (for momentum channels $0 \rightarrow 1$ and $1 \rightarrow 0$) and $A_1/2iT_2$ (for momentum channels $0 \rightarrow 0$ and $1 \rightarrow 1_\perp$) for different pseudoscalar meson masses, allowing for linear and quadratic $1/M$ corrections to the infinite mass limit predictions of equation (12). The linear and quadratic extrapolations in $1/M$ agree within errors for the extrapolated values, with the exception of three cases of the infinite mass limit points (one of which is shown in figure 2). We trust the linear extrapolations more than the quadratic ones: we are fitting to four points only in a limited region of inverse heavy-light pseudoscalar mass, and quadratic fits can amplify accidental quadratic effects in the fitted points. All results in the remainder of this section will refer to linear extrapolations.

Figure 3 shows the ratios $V/2T_1$ and $A_1/2iT_2$ for five values of ω at three different heavy-light pseudoscalar masses, around the D mass, around the B mass and in the infinite mass limit. The results around the D mass are our measured values at $\kappa_h = 0.129$ (which corresponds very closely to the charm quark). The B mass and infinite mass limit results are extrapolations. The HQS predictions of equation (12) are well satisfied for both ratios in the infinite mass limit. The ratio $V/2T_1$ shows large $1/M$ corrections of the order of 75% at the D scale and 20% at the B scale. Corrections of about 30% at the D scale and about 10% at the B scale were previously observed for the pseudoscalar meson decay constant f_P [39] and for the form factor h_V in heavy-to-heavy $0^- \rightarrow 1^-$ semileptonic decays [16]⁶. In contrast, the ratio $A_1/2iT_2$ exhibits small $1/M$ corrections even at the D meson scale. A similar situation occurs for the form factors h_+ and h_{A_1} in heavy-to-heavy $0^- \rightarrow 0^-, 1^-$ semileptonic decays [15, 16]⁷.

⁵ $A_1(q_{\text{max}}^2)$ and $T_2(q_{\text{max}}^2)$ can be determined directly from the $0 \rightarrow 0$ data, but $V(q_{\text{max}}^2)$ and $T_1(q_{\text{max}}^2)$ have to be obtained by an extrapolation in q^2 from the measured data.

⁶Short distance corrections have been accounted for in the form factors h_V , h_+ and h_{A_1} .

⁷Note that h_+ and h_{A_1} are protected from $1/M$ corrections at zero recoil by Luke's theorem [40] and the leading corrections are of order $1/M^2$.

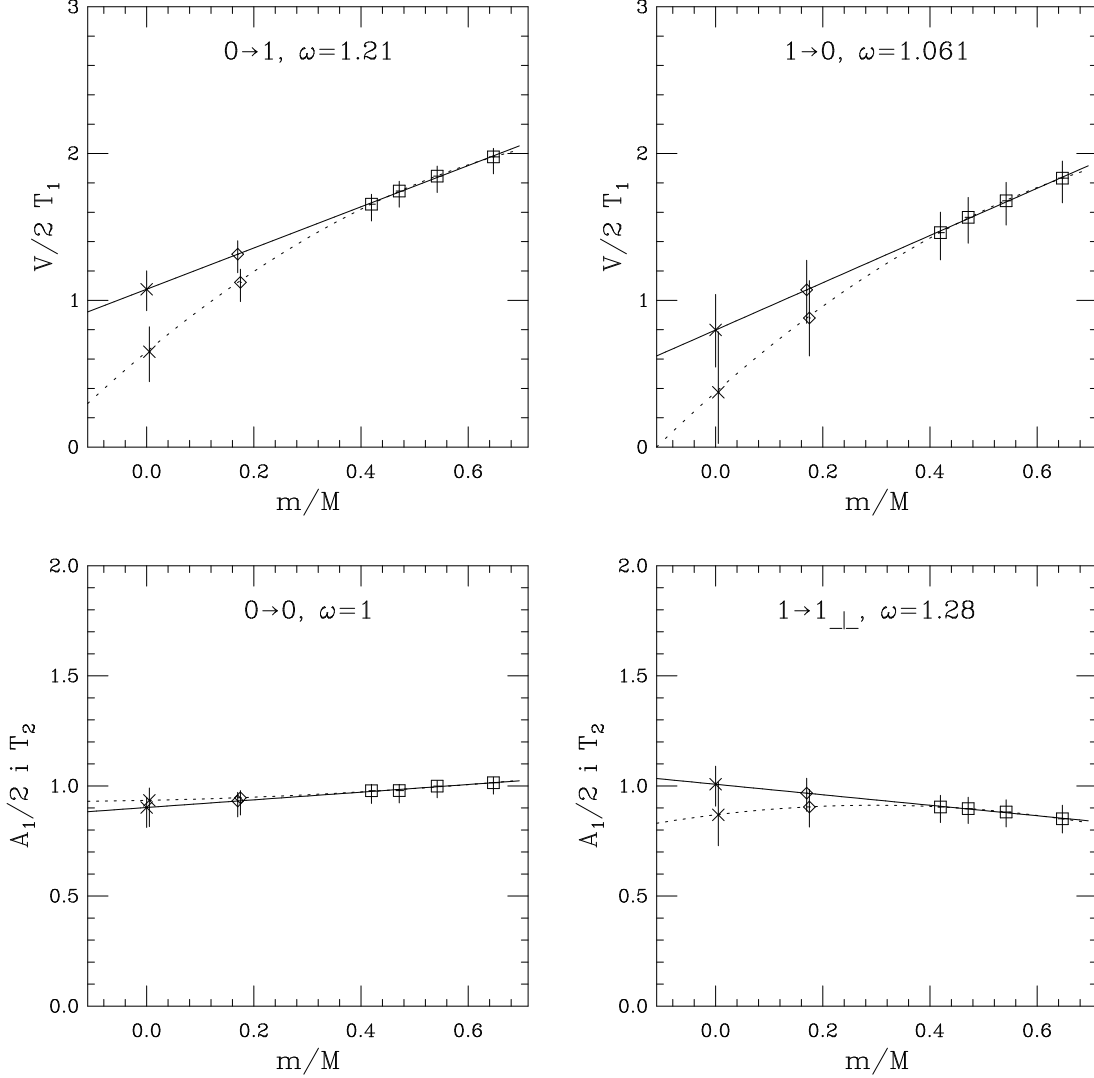


Figure 2 $V/2T_1$ and $A_1/2iT_2$ as a function of the ratio of the light vector meson mass over the heavy-light pseudoscalar meson mass, for different heavy quark masses (squares) and various momentum channels. For the $0 \rightarrow 0$ channel ω is 1 exactly. For the remaining channels, the value of ω shown in each plot has an error of less than 1 in the last digit. We show both linear (solid) and quadratic (dashed) extrapolations in $1/M$. The extrapolations to the B scale and the infinite mass limit are indicated by diamonds and crosses respectively.

Inclusion of kinematic $1/M$ factors, as shown in equations (14) and (15) reduces the size of the $1/M$ corrections by about a factor of two for the relation between T_1 and V , giving results in agreement with those in reference [41], but has little effect on the T_2 and A_1 relation (note that the T_2 - A_1 relation in equa-

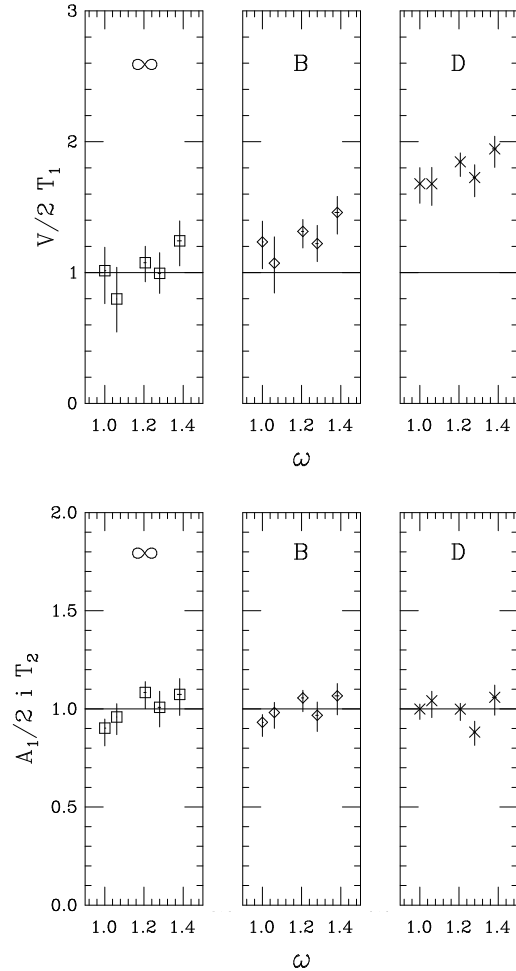


Figure 3 Ratios $V/2T_1$ and $A_1/2iT_2$ for five values of ω at three different heavy-light pseudoscalar masses, around the D mass (crosses), around the B mass (diamonds) and in the infinite mass limit (squares). The horizontal solid line denotes the HQS prediction in the infinite mass limit.

tion (15) reduces to the result in equation (12) at $\omega = 1$).

5 Cabibbo Suppressed Decays

For this exploratory study we did not have a complete set of light quark kappa values for every heavy-quark kappa value, as discussed in section 3. This prevented us, in [36], from performing a reliable chiral extrapolation to obtain results for the semileptonic decay $\bar{B}^0 \rightarrow \pi^+ l^- \bar{\nu}_l$. Here we are concerned with semileptonic decays with a light vector meson in the final state: in contrast to the case of a pion, which is a pseudo-Goldstone boson, we do not expect a sizable effect

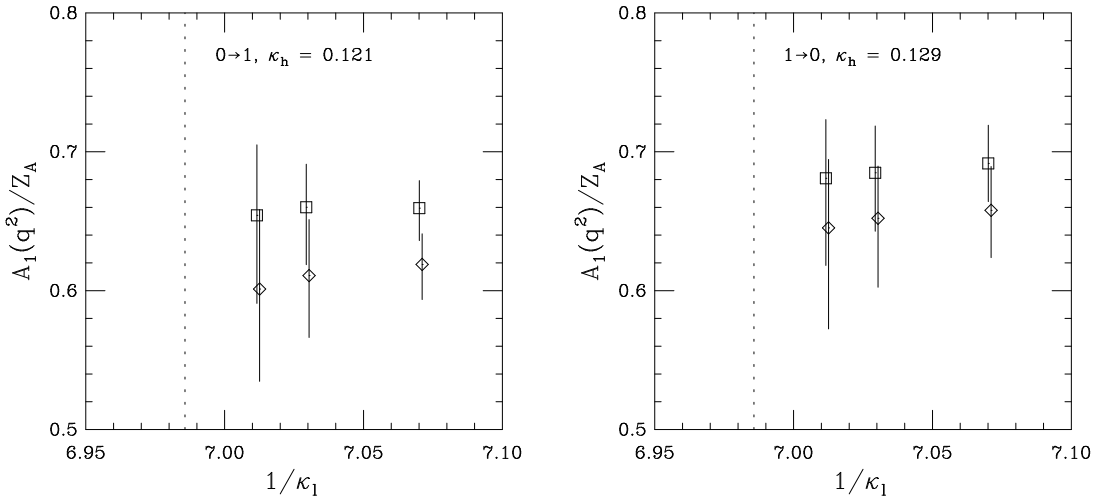


Figure 4 A_1/Z_A for two different momentum channels and six different combinations of spectator and active quark masses as a function of the inverse spectator quark kappa value. Squares denote $\kappa_a = 0.14144$ and diamonds denote $\kappa_a = 0.14226$. The diamond points are slightly displaced horizontally for clarity. The heavy kappa values are $\kappa_h = 0.121$ for the $0 \rightarrow 1$ channel and 0.129 for the $1 \rightarrow 0$ channel. The vertical dashed line marks the chiral limit for the light spectator quark.

from the chiral extrapolation.

Indeed, in figure 4 we show the dependence of the form factor A_1 on the active and spectator light-quark masses, for two different combinations of momentum channel and heavy quark mass, $\kappa_h = 0.121$ and 0.129 , for which six combinations of light quark kappas were computed. It can be seen that in both cases A_1 remains practically constant as the light spectator quark mass decreases (horizontal movement on the plots) but there is a dependence on the active quark mass (vertical movement). Note that the value of ω , and hence q^2 , depends on κ_l as well as κ_a , and therefore the results of figure 4 indicate that $A_1^{\kappa_l, \kappa_a}(\omega(\kappa_l, \kappa_a))$ is nearly independent of κ_l , in which case,

$$A_1^{\kappa_{\text{crit}}, \kappa_{\text{crit}}}(\omega(\kappa_{\text{crit}}, \kappa_{\text{crit}})) \approx A_1^{\kappa_l=0.14144, \kappa_{\text{crit}}}(\omega(\kappa_l=0.14144, \kappa_{\text{crit}})). \quad (19)$$

Similar independence of the spectator mass was found in the study of the form factor T_2 in the radiative decay $\bar{B} \rightarrow K^* \gamma$ [32]. As we have shown in the previous section, A_1 is equal to $2iT_2$ to good approximation for different heavy quark masses and different momentum channels and therefore the results of [32] give us further evidence of the spectator mass independence of A_1 .

The situation is less clear for the form factors A_2 and V owing to the larger statistical errors. A_2 and V appear to follow the same pattern as A_1 , but we cannot dismiss a possible mild dependence on the light spectator mass. In figure 5 we show two examples of the dependence of the form factors V and A_2 on the active and spectator light quark masses.

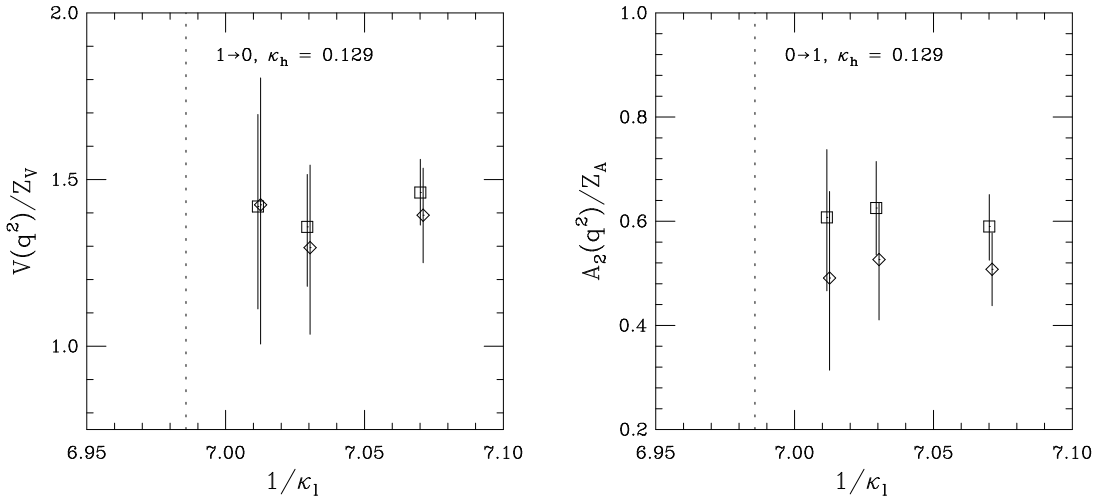


Figure 5 $V(q_{1\rightarrow 0}^2)/Z_V$ and $A_2(q_{0\rightarrow 1}^2)/Z_A$ for two different momentum channels and six different combinations of spectator and active quark masses as a function of the inverse spectator quark kappa value. Squares denote $\kappa_a = 0.14144$ and diamonds denote $\kappa_a = 0.14226$. The diamond points are slightly displaced horizontally for clarity. The heavy kappa value is $\kappa_h = 0.129$ in both cases. The vertical dashed line marks the chiral limit for the light spectator quark.

We are going to assume the form factors are independent of the light spectator mass, and therefore we will extrapolate to the chiral limit only for the active light quark, as was suggested for A_1 in equation (19). This will allow us to use results for all four heavy quark masses to guide our extrapolations to the B mass. To quantify the systematic error induced we have compared, for the two heavy kappa values for which we have six combinations of light quark masses, the chiral-extrapolated form factor values for each momentum channel using two procedures:

1. Using all six data points we can extrapolate to the chiral limit for both the spectator and active quarks (see reference [33]).
2. Fixing the spectator kappa value to 0.14144 and assuming complete independence of the form factors on the spectator quark mass, we perform the chiral extrapolation for the active quark only, as indicated in equation (19) for A_1 .

For A_1 the two procedures give the same results within 5% except for those channels involving a momentum of $\sqrt{2}$ in lattice units for the light vector meson, where the variation can be 10%. These errors are comparable with the statistical ones. For procedure 1 above, the chiral extrapolation for the $\sqrt{2}$ channels is less reliable than for channels with lower light meson momentum, because the statistical fluctuations for three-point functions with the lightest light-quark masses

channel	q^2 / GeV^2	A_1	A_2	V
$0 \rightarrow 0$	20.3	0.46_{-3}^{+2}	—	—
$0 \rightarrow 1$	17.5_{-2}^{+2}	0.43_{-2}^{+2}	0.8_{-2}^{+2}	1.6_{-1}^{+1}
$0 \rightarrow \sqrt{2}$	15.3_{-3}^{+3}	0.39_{-2}^{+3}	0.7_{-1}^{+2}	1.2_{-1}^{+1}
$1 \rightarrow 0$	19.7_{-1}^{+1}	0.46_{-3}^{+3}	—	—
$1 \rightarrow 1_{\perp}$	16.7_{-2}^{+2}	0.38_{-3}^{+3}	0.6_{-3}^{+3}	1.5_{-2}^{+2}
$1 \rightarrow \sqrt{2}_{\perp}$	14.4_{-3}^{+3}	0.39_{-5}^{+6}	0.7_{-2}^{+3}	1.4_{-2}^{+3}

Table 1 Values of the form factors for $\bar{B}^0 \rightarrow \rho^+ l^- \bar{\nu}_l$ for different values of q^2 close to q_{max}^2 . For the $0 \rightarrow 0$ channel, ω is 1 exactly, so that q^2 is fixed up to (tiny) experimental errors in the physical meson masses. For A_2 and V , the zero recoil channel, $0 \rightarrow 0$ is not measured. In addition, the large statistical errors in A_2 and V for the $1 \rightarrow 0$ channel prevent a reliable extrapolation in $1/M$. Quoted errors are purely statistical. Adding systematic errors from spectator quark flavour symmetry breaking and discretisation in quadrature produces a further 11% error in A_1 , 20% in A_2 and 15% in V .

($\kappa_l = 0.14226, 0.14262$) are larger. These fluctuations can account for an important part of the 10% variation observed between the two procedures. We have decided to use 5% to estimate, for all momentum channels, the systematic error on A_1 induced by this assumption of independence of the light spectator quark mass.

The statistical fluctuations are much larger for A_2 and V , making it difficult to check the difference between the results from the two chiral extrapolation procedures above. We will adopt a conservative position and will admit a 20% systematic error in A_2 and a 10% error in V , based on the maximum discrepancies observed between the two procedures. These discrepancies are within the statistical error bars.

In figure 6 we show extrapolations to the B mass scale for the form factors A_1 , A_2 and V , allowing for linear and quadratic $1/M$ corrections to the infinite mass limit predictions of equation (10). The extrapolated values agree well for the linear and quadratic fits: we will quote results only from the linear fits in the following, unless stated otherwise. We have used six momentum channels: the same five channels used in the previous section together with the channel $1 \rightarrow \sqrt{2}_{\perp}$. For A_2 and V the momentum channels $0 \rightarrow 0$ and $1 \rightarrow 0$ are extremely noisy and we cannot control the extrapolations⁸. The measured values of the form factors, extrapolated to the B scale for different values of q^2 close to q_{max}^2 , are listed in table 1.

In figure 7a we show $A_1(q^2)$ at the B scale, together with three fits to its q^2

⁸The $0 \rightarrow 0$ momentum channel is not measured directly for A_2 and V .

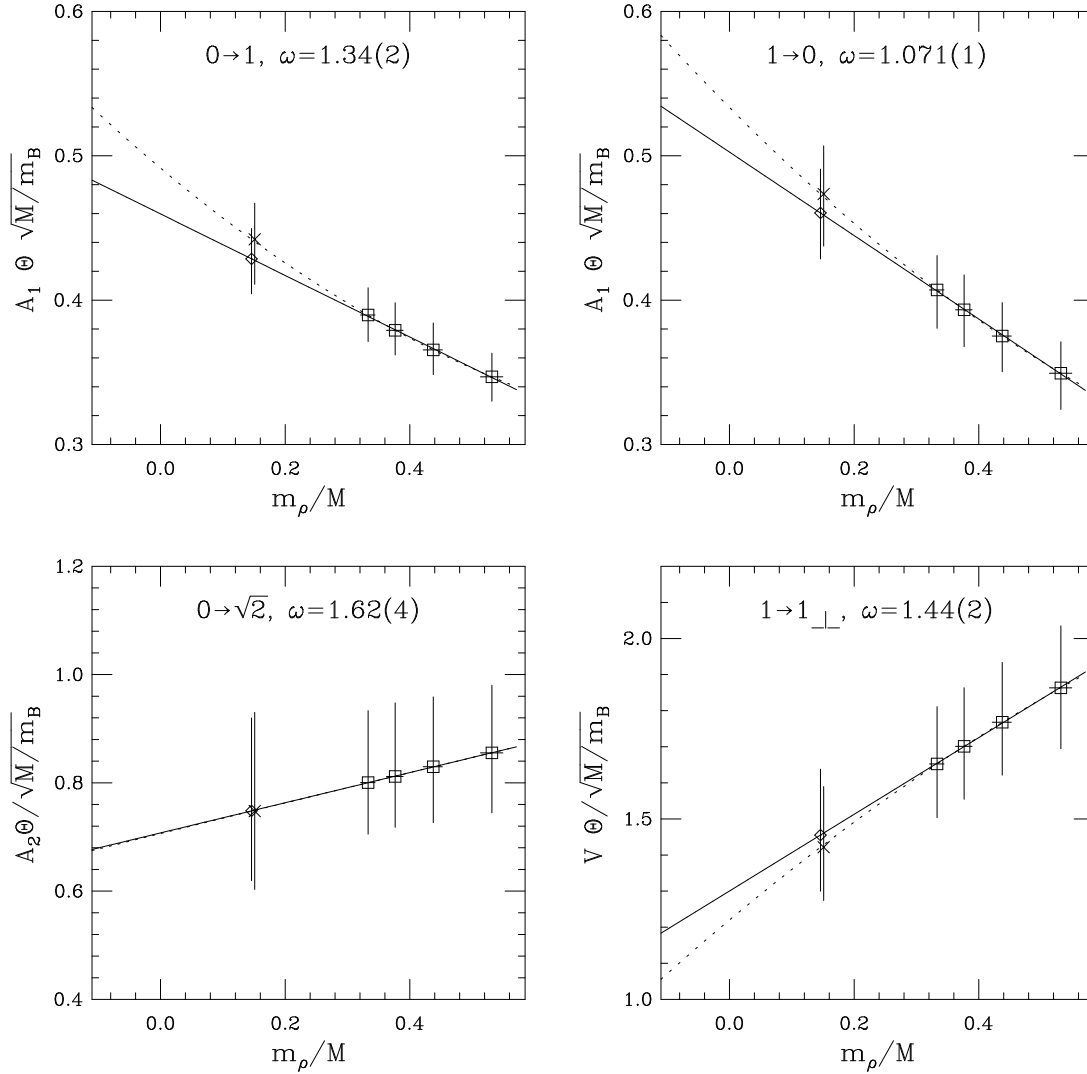


Figure 6 Linear (solid line) and quadratic (dashed line) $1/M$ extrapolations of A_1 , A_2 and V in selected momentum channels as functions of m_ρ/M . Squares denote measured points. Diamonds and crosses mark the extrapolations to the B scale for the linear and quadratic fits respectively.

dependence:

$$A_1(q^2) = \begin{cases} A_1(0) & \text{constant,} \\ \frac{A_1(0)}{1 - q^2/m_{\text{pole}}^2} & \text{pole,} \\ \frac{A_1(0)}{(1 - q^2/m_{\text{dipole}}^2)^2} & \text{dipole.} \end{cases} \quad (20)$$

Table 2 shows the fit parameters for each q^2 dependence, with the corresponding

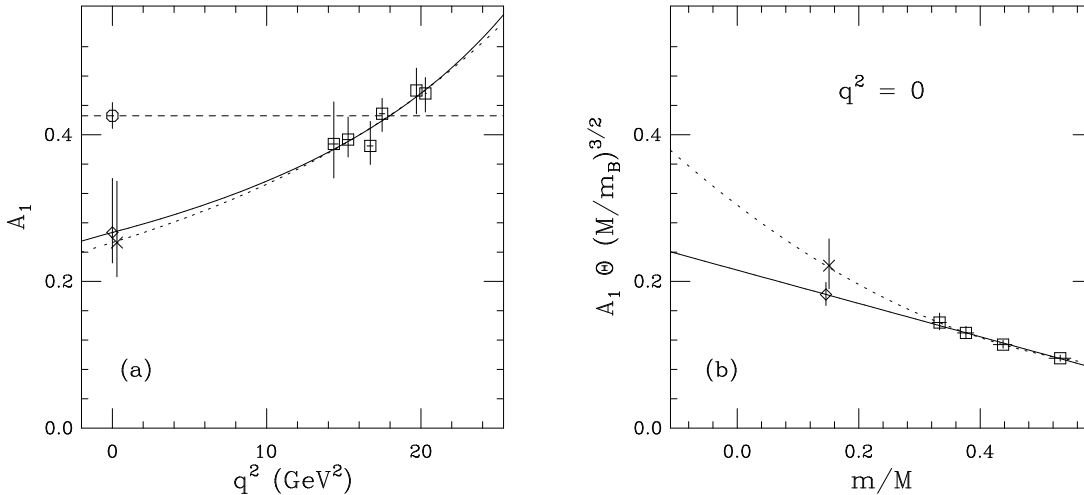


Figure 7 (a): form factor $A_1(q^2)$ for the decay $\bar{B}^0 \rightarrow \rho^+ l^- \bar{\nu}_l$. Squares are measured data extrapolated to the B scale at fixed ω . The three curves and points at $q^2 = 0$ have been obtained by fitting the squares using the q^2 dependences from equation (20): constant (dashed line and octagon), pole (solid line and diamond) and dipole (dotted line and cross). The point at $q^2 = 0$ for the dipole fit has been displaced slightly for clarity. **(b):** linear (solid) and quadratic (dashed) extrapolations of $A_1(0)$ in $1/M$ to the B scale according to equation (21). Squares are obtained from pole fits to the measured data for the different heavy quark kappa values. The diamond and cross give the form factor at the B scale.

fit type	$A_1(0)$	$m_{\text{pole}}/\text{GeV}$	$m_{\text{dipole}}/\text{GeV}$	χ^2/dof
constant	0.43^{+2}_{-2}	—	—	1.3
pole	0.27^{+7}_{-4}	7^{+2}_{-1}	—	0.2
dipole	0.25^{+8}_{-5}	—	9^{+4}_{-1}	0.2

Table 2 Fit parameters for different q^2 dependences for the form factor $A_1(q^2)$ at the B scale. Quoted errors are statistical only.

χ^2 per degree of freedom.

The figure and table indicate that constant-in- q^2 behaviour for A_1 does not fit the data well. This feature is even more evident in lattice studies at the D scale, where fits to constant behaviour are poor [33]–[35], [42, 43]. Our data favour a pole type behaviour with a pole mass in the expected range for a $1^+ b\bar{u}$ resonance [43]. Dipole (and in general higher powers: tripole, ...) and pole fits are hardly distinguishable in the physical range $0 \leq q^2 \leq q_{\text{max}}^2$. In a dipole fit, the mass parameter m_{dipole} is roughly given by $m_{\text{dipole}} \approx \sqrt{2}m_{\text{pole}}$ and hence pole and dipole fits agree in the limited range of values of q^2 , well below m_{pole}^2 , explored in figure 7a. An alternative procedure is to use pole fits for extracting

$A_1(\kappa_h; q^2=0)$ from our measured data, at different heavy quark masses around that of the charm and then to extrapolate $A_1(0)$ in $1/M$ to the B scale, as shown in figure 7b, by using [32, 36, 44]

$$A_1(0)\Theta M^{3/2} = \text{const}(1 + \gamma/M + \delta/M^2 + \dots). \quad (21)$$

This gives a result for $A_1(0)$ at the B scale (using linear or quadratic extrapolations in $1/M$) of,

$$A_1(q^2=0; m_B) = \begin{cases} 0.18 \pm 0.02 & \text{linear} \\ 0.22^{+4}_{-3} & \text{quadratic} \end{cases}. \quad (22)$$

The quoted errors are purely statistical. A further 11% systematic error should be added, obtained by combining in quadrature the systematic errors from the spectator quark flavour symmetry breaking and discretisation effects. Incorporating the systematic error makes this method of extracting $A_1(0)$ consistent within errors with the method presented in table 2.

In conclusion, we find that $A_1(q^2)$ at the B scale is fitted by a single pole form, with the parameters given in table 2. The errors in table 2 are statistical only: as mentioned above, a further 11% systematic error should be added. In table 3 we compare our results with other theoretical calculations: the agreement is generally good. Previous lattice results [42, 43] rely on the assumption of pole behaviour using a lattice determination of the $b\bar{u}$ 1^+ resonance (\bar{B}_1) mass and the value of $A_1(q^2)$ at a *single* q^2 value. In contrast, in this paper, we have tried to determine the q^2 dependence of A_1 .

Statistical and systematic uncertainties in the present study have prevented us from extracting the q^2 dependence of the A_2 and V form factors.

Much effort has recently been devoted by the lattice community to determining the q^2 behaviour of T_1 and T_2 around the B scale, without producing a definitive conclusion. The q^2 dependence found here for A_1 and the results from the previous section for the ratio $A_1/2iT_2$ may support a pole-type behaviour for T_2 at least in a region around q_{max}^2 . Sum-rules calculations [41, 45, 46] and a recent calculation by B Stech [49] find that V has a more pronounced q^2 dependence than A_1 , which is consistent with having dipole type behaviour for V and pole behaviour for A_1 . In the previous section we found that around the B scale T_1 is roughly equal to V . This supports a dipole behaviour for T_1 and consequently further favours a pole behaviour for T_2 [32, 36, 44].

6 Extraction of $|V_{ub}|$

In this section we employ our lattice determination of the form factors to calculate the differential decay rate $d\Gamma/dq^2$ for the decay $\bar{B}^0 \rightarrow \rho^+ l^- \bar{\nu}_l$ in the region near q_{max}^2 . Experimental data for this region will enable a model-independent determination of $|V_{ub}|$.

Reference	$A_1(0)$
This work	0.27_{-4-3}^{+7+3}
ELC “a” [42]	0.25 ± 0.06
ELC “b” [42]	0.22 ± 0.05
APE “a” [43]	0.29 ± 0.16
APE “b” [43]	0.24 ± 0.12
Sum rules [41]	0.24 ± 0.04
Sum rules [45]	0.5 ± 0.1
Sum rules [46]	0.35 ± 0.16
Quark model [6]	0.05
Quark model [7]	0.28
Quark model [47]	0.26 ± 0.03
HQS & χ PT [48]	0.21

Table 3 Values for $A_1(0)$ for $\bar{B}^0 \rightarrow \rho^+ l^- \bar{\nu}_l$ from various theoretical calculations. The second set of errors in our quoted value denotes our estimate of systematic effects from the spectator quark flavour symmetry breaking and discretisation.

It has previously been suggested that determinations of the decay rate for $\bar{B}^0 \rightarrow \rho^+ l^- \bar{\nu}_l$ near $q^2 = 0$, combined with the experimentally-measured branching fractions $B(\bar{B} \rightarrow K^* \gamma)$ and $B(b \rightarrow s \gamma)$ would also allow a determination of $|V_{ub}|$. However, one method relies on three different measurements, $B(\bar{B} \rightarrow K^* \gamma)$, $B(b \rightarrow s \gamma)$ and $d\Gamma(\bar{B}^0 \rightarrow \rho^+ l^- \bar{\nu}_l)/dq^2|_{q^2=0}$, together with the theoretical determination of the ratio $T_1^{\bar{B} \rightarrow K^* \gamma}(0)/A_0^{B \rightarrow \rho}(0)$ [22, 23]. The evaluation of this ratio of form factors from lattice calculations involves difficult and model-dependent extrapolations from the vicinity of q_{\max}^2 to $q^2 = 0$. Another method uses the ratio of $\Gamma(\bar{B} \rightarrow K^* \gamma)$ and $\lim_{q^2 \rightarrow 0} d\Gamma(\bar{B}^0 \rightarrow \rho^+ l^- \bar{\nu}_l)/dE_\rho dE_l$ evaluated on a curve where $q^2 = 4E_l(m_B - E_\rho - E_l)$ [21], which is independent of any hadronic form factor. However, it relies on the validity of the leading order HQS relations of equations (14) and (15) between the form factors for the radiative and semileptonic decays in the region around $q^2 = 0$, far from the zero recoil point. Furthermore, light flavour $SU(3)$ symmetry is used to relate the K^* and the ρ mesons. Corrections to these approximations will induce systematic errors in the determination of $|V_{ub}|$. For example, the sum rule calculation of the relevant form factors in reference [41] finds about 7% corrections to the leading HQS relations and about 25% corrections from $SU(3)$ breaking.

We propose to look at the region around q_{\max}^2 for the process $\bar{B}^0 \rightarrow \rho^+ l^- \bar{\nu}_l$, beyond the region of charm production which complicates the experimental determination of $b \rightarrow u$ transitions at low q^2 (note that $|V_{ub}/V_{cb}|^2$ determined from inclusive decays is expected to be less than 0.01). The methods referred to above, based on determinations of the decay rate near $q^2 = 0$, suffer from this experimen-

tal difficulty in addition to possible theoretical uncertainties. Lattice techniques, in contrast, allow the form factors to be measured directly near q_{max}^2 , using only a $1/M$ extrapolation motivated by HQS, and avoiding the problematic model-dependent extrapolation to $q^2 = 0$. This model-dependence currently plagues the lattice determination of $B(\bar{B} \rightarrow K^* \gamma)$ which requires knowledge of the form factors T_1 and/or T_2 at $q^2 = 0$, where they are equal.

The differential decay rate for $\bar{B}^0 \rightarrow \rho^+ l^- \bar{\nu}_l$ is given by

$$\frac{d\Gamma(\bar{B}^0 \rightarrow \rho^+ l^- \bar{\nu}_l)}{dq^2} = \frac{G_F^2 |V_{ub}|^2}{192\pi^3 m_B^3} q^2 [\lambda(q^2)]^{\frac{1}{2}} \times \left(|H^+(q^2)|^2 + |H^-(q^2)|^2 + |H^0(q^2)|^2 \right) \quad (23)$$

where $\lambda(q^2) = (m_B^2 + m_\rho^2 - q^2)^2 - 4m_B^2 m_\rho^2$. H^0 comes from the contribution of the longitudinally polarised ρ and is given by

$$H^0(q^2) = \frac{-1}{2m_\rho \sqrt{q^2}} \left\{ (m_B^2 - m_\rho^2 - q^2)(m_B + m_\rho) A_1(q^2) - \frac{4m_B^2 |\mathbf{k}|^2}{m_B + m_\rho} A_2(q^2) \right\}, \quad (24)$$

where \mathbf{k} is the momentum of the ρ in the B -meson rest frame. H^\pm correspond to the contribution of the transverse polarisations of the vector meson and are given by

$$H^\pm(q^2) = - \left\{ (m_B + m_\rho) A_1(q^2) \mp \frac{2m_B |\mathbf{k}|}{(m_B + m_\rho)} V(q^2) \right\}. \quad (25)$$

Looking for semileptonic decays beyond the charm production threshold (determined by the semileptonic $\bar{B} \rightarrow Dl\bar{\nu}_l$ decay) will make sense only if there are enough events. In figure 8 we show the differential decay rates $d\Gamma/dq^2$ for $\bar{B}^0 \rightarrow \rho^+ l^- \bar{\nu}_l$ and $\bar{B}^0 \rightarrow \pi^+ l^- \bar{\nu}_l$. For $\bar{B}^0 \rightarrow \rho^+ l^- \bar{\nu}_l$ we assume that A_1 , A_2 and V are all given by single pole forms with a common pole mass of 5.3 GeV and a normalisation determined by our measurements for the $0 \rightarrow 1$ momentum channel. For $\bar{B}^0 \rightarrow \pi^+ l^- \bar{\nu}_l$ we use the results of reference [36] with a dipole form for the form factor f^+ with $f^+(0) = 0.24$ and a mass parameter $m_{f^+} = 5.7$ GeV. These curves are meant to be illustrative, based on reasonable hypotheses: for $\bar{B}^0 \rightarrow \pi^+ l^- \bar{\nu}_l$ the results in [36] were obtained for unphysically large u and d quark masses; for $\bar{B}^0 \rightarrow \rho^+ l^- \bar{\nu}_l$ we do not necessarily believe that the three form factors involved are all simultaneously single pole types with the same pole mass (the pole mass of 5.3 GeV is an estimate of the average of the 1^- and 1^+ $b\bar{u}$ resonance masses). The points we wish to make are:

1. For $\bar{B}^0 \rightarrow \rho^+ l^- \bar{\nu}_l$ the events near $q^2 = 0$ have already been recommended for study, but the expected number of events at large q^2 is at least comparable.
2. In the region beyond the charm threshold, the rates for $\bar{B}^0 \rightarrow \rho^+ l^- \bar{\nu}_l$ and $\bar{B}^0 \rightarrow \pi^+ l^- \bar{\nu}_l$ are at least comparable ($\bar{B}^0 \rightarrow \pi^+ l^- \bar{\nu}_l$ is not ten times more

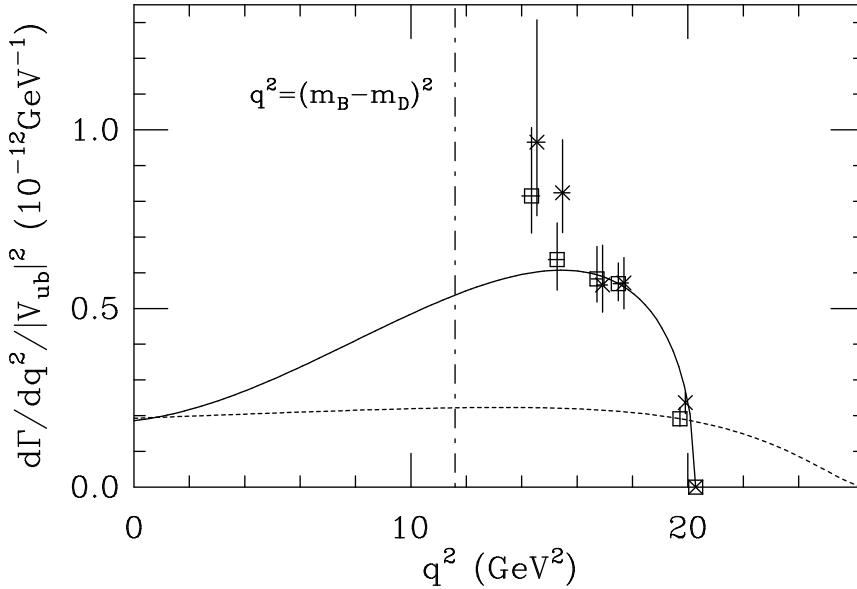


Figure 8 Differential decay rates for $\bar{B}^0 \rightarrow \rho^+ l^- \bar{\nu}_l$ and $\bar{B}^0 \rightarrow \pi^+ l^- \bar{\nu}_l$. The data points and solid curve are for $\bar{B}^0 \rightarrow \rho^+ l^- \bar{\nu}_l$: squares have contributions from our measured values for A_1 , A_2 and V , crosses have A_1 only, and the crosses are offset slightly for clarity. The dashed curve is for $\bar{B}^0 \rightarrow \pi^+ l^- \bar{\nu}_l$. The curves are illustrative, as described in the text. The vertical dot-dashed line marks the upper limit in q^2 for charm production.

common than $\bar{B}^0 \rightarrow \rho^+ l^- \bar{\nu}_l$, for example), so both should be sizable contributions to the inclusive $b \rightarrow u$ event rate and either or both can be used for the determination of $|V_{ub}|$.

The lattice calculations of the form factors in the previous section provide data points for $d\Gamma/dq^2$ over a sizable fraction of the region in q^2 above the charm endpoint, as can be seen in figure 8. The uncertainties in determining A_2 and V in the $0 \rightarrow 0$ and $1 \rightarrow 0$ momentum channels do not prejudice our measurement of the differential decay rate. The rate is forced to vanish for kinematical reasons at q_{\max}^2 so the $0 \rightarrow 0$ channel form factor values of A_2 and V are irrelevant. Moreover, the contribution to the differential decay rate of these two form factors in the $1 \rightarrow 0$ channel is highly suppressed (the $1 \rightarrow 0$ channel has a q^2 near q_{\max}^2 and the A_2 and V contributions are suppressed relative to that of A_1 by a factor \mathbf{k}^2/m_B^2 as shown in equation (23)). Over the range of q^2 for which we have measurements, the differential decay rate is dominated by the form factor A_1 . This is shown by the difference between the points marked by squares and crosses in figure 8.

In table 4 we give the numerical values we have obtained for the differential decay rate at several q^2 values. We have parametrised the results of the table by

q^2	$d\Gamma/dq^2$	$\int_{q^2}^{q_{\max}^2} dq^2 d\Gamma/dq^2$
20.3	0.0	0.0
19.7_{-1}^{+1}	0.19_{-2}^{+3}	0.08_{-1}^{+1}
17.5_{-2}^{+2}	0.57_{-5}^{+6}	0.9_{-1}^{+1}
16.7_{-2}^{+2}	0.58_{-6}^{+9}	1.3_{-1}^{+1}
15.3_{-3}^{+3}	0.6_{-1}^{+1}	2.3_{-2}^{+2}
14.4_{-3}^{+3}	0.8_{-1}^{+2}	3.0_{-2}^{+3}
charm threshold		
11.6	—	5.4_{-5}^{+7}

Table 4 Differential and partially integrated decay rate for $\bar{B}^0 \rightarrow \rho^+ l^- \bar{\nu}_l$ measured on the lattice for various q^2 values. q^2 is given in units of GeV^2 and Γ in units of $|V_{ub}|^2 10^{-12} \text{ GeV}$. For the $0 \rightarrow 0$ channel, ω is 1 exactly, so that q^2 is fixed up to (tiny) experimental errors in the physical meson masses. The integration has been performed using the parametrisation of equation (26). Quoted errors are purely statistical — a further 24% systematic error should be added as discussed in the text.

fitting our measured points for $d\Gamma/dq^2$ to the form

$$\frac{10^{12}}{|V_{ub}|^2} \frac{d\Gamma(\bar{B}^0 \rightarrow \rho^+ l^- \bar{\nu}_l)}{dq^2} = \frac{G_F^2}{192\pi^3 m_B^3} q^2 [\lambda(q^2)]^{\frac{1}{2}} a^2 (1 + b(q^2 - q_{\max}^2)), \quad (26)$$

obtained by retaining the phase space dependence and expanding H^\pm and H^0 from equation (23) around q_{\max}^2 . The results of the fit are

$$\begin{aligned} a^2 &= 21_{-3}^{+3} \text{ GeV}^2, \\ b &= (-8_{-6}^{+4}) 10^{-2} \text{ GeV}^{-2}, \end{aligned} \quad (27)$$

where the quoted errors are statistical. A 24% systematic error should be added as discussed below.

With this parametrisation, we can partially integrate the differential decay rate, giving the results shown in the last column of table 4. The table also includes the partially integrated decay rate from the charm threshold to q_{\max}^2 , although higher order terms in the Taylor expansion in equation (26) could become sizable at the lower end of this range, where we do not currently have measured points. The results of table 4 and equation (27) have been obtained by extrapolating the form factors linearly in $1/M$. Quadratic extrapolations in $1/M$ give results differing in the last significant figure, which is always well within the statistical errors. In figure 9 we show our measured data together with the fit, including 68% confidence level bounds.

Comparison of any of the values in table 4 with experimental measurements will allow an extraction of $|V_{ub}|$ with less than 10% statistical and 12% systematic

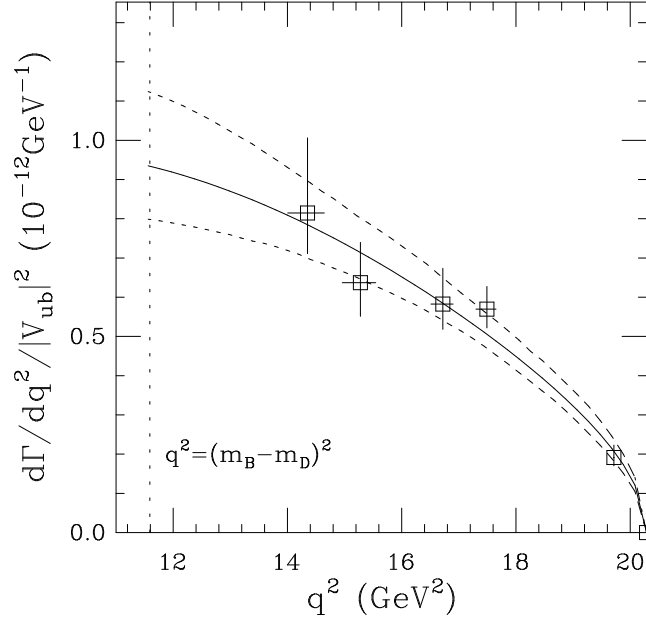


Figure 9 Differential decay rate as a function of q^2 for the semileptonic decay $\bar{B}^0 \rightarrow \rho^+ l^- \bar{\nu}_l$. Squares are measured lattice data, solid curve is fit from equation (26) with the parameters given in equation (27). Dashed lines are 68% confidence limits (statistical errors only). The vertical dotted line marks the charm threshold.

theoretical uncertainties. Another way to determine $|V_{ub}|$ uses the parametrisation of equation (26) and our results of equation (27). It parallels the method used to extract $|V_{cb}|$ from semileptonic $\bar{B} \rightarrow D^*$ decays (see references [13]–[19]). The factor $a^2(1 + b(q^2 - q_{\max}^2))$ in equation (26) parametrises long distance hadronic dynamics (it is the analogue of the function $\hat{\xi}^2(\omega)$ in [13] for the $\bar{B} \rightarrow D^*$ case). The idea is to use experimental measurements of $d\Gamma/dq^2$ extrapolated to q_{\max}^2 to extract a value for $|V_{ub}|^2 a^2$ and compare with our theoretical determination of a^2 . Here a plays the role of $\hat{\xi}(1)$ in the $\bar{B} \rightarrow D^*$ extraction of $|V_{cb}|$.

The lattice simulation provides a systematic determination of the overall normalisation of hadronic dynamical effects, parametrised by a . For the extraction of $|V_{cb}|$ from $\bar{B} \rightarrow D^*$ decays HQS provides such a normalisation (the Isgur-Wise function is 1 at zero recoil, up to $1/M^2$ and short distance perturbative corrections). For the heavy-to-light $\bar{B}^0 \rightarrow \rho^+ l^- \bar{\nu}_l$ semileptonic decay, such a normalisation is not provided by HQS.

In the fit to equation (26) the $0 \rightarrow 0$ channel is not used because $d\Gamma/dq^2|_{q_{\max}^2}$ is zero and our fitting function automatically incorporates this feature. Our value for $A_1(q_{\max}^2)$ from the $0 \rightarrow 0$ channel therefore gives an independent measurement of a^2 because V and A_2 do not contribute at this kinematic point. We find, using

the value from table 1, and quoting statistical errors only,

$$a^2 = 3(m_B + m_\rho)^2 A_1^2(q_{\max}^2) = 23_{-2}^{+2} \text{ GeV}^2, \quad (28)$$

in excellent agreement with a^2 determined by the fit to the other channels. This suggests that discretisation and other systematic errors have not conspired to change drastically the shape of the overall q^2 dependence. Our final result will use the value of a^2 , given in equation (27), determined from the fit to these other channels, because this does not rely on a single measurement.

To estimate systematic uncertainties, we have considered four possible sources of errors: quenching, determination of the lattice spacing in physical units, light spectator mass independence of the form factors and discretisation errors.

The exact effect of ignoring internal quark loops is an unknown systematic error. However, quenched lattice calculations of form factors for $D \rightarrow K, K^*$ semileptonic decays (see [33] and references therein) give results in agreement with world average experimental values, while quenched calculations of $\bar{B} \rightarrow D, D^*$ [15] decays have allowed extractions of $|V_{cb}|$ in agreement with other determinations of that quantity. This gives us some confidence that errors due to quenching are most likely within the statistical errors for processes involving a heavy quark.

The error arising from uncertainties in the value of the lattice spacing in physical units should be minimised in our calculation, because we have evaluated only dimensionless quantities: form factors and values of the velocity transfer, $\omega = v \cdot v'$. Physical meson masses have been used as input where dimensional results are required. The only dependence on the lattice scale enters in expressing the heavy-light pseudoscalar masses in physical units for the $1/M$ extrapolations of the form factors and in the short distance logarithmic corrections of equation (11). The systematic error induced is much smaller than the other errors we will consider below.

We believe our results show good evidence for light spectator mass independence of the form factors. We made this independence an assumption in order to use the results for the heaviest light spectator quark only: these results have smaller statistical error and are available for all our heavy quarks. In the previous section we argued that we could not rule out a 5% error in A_1 (10% in channels involving $\sqrt{2}$ momenta for the light meson) due to this assumption. The corresponding errors in A_2 and V were 20% and 10% respectively. In the region near q_{\max}^2 , $d\Gamma/dq^2$ is dominated by A_1 and the contributions of V and A_2 are kinematically suppressed, being 5% or less for $q^2 > 16 \text{ GeV}^2$. The $0 \rightarrow \sqrt{2}$ and $1 \rightarrow \sqrt{2}$ channels explore lower q^2 values where the V and A_2 contributions are less suppressed, of order 15–20% (see figure 8). If the spectator quark mass independence assumption were violated by as much as 20% for V and A_2 , the error in the differential decay rate would only be of the order of 2% for the non- $\sqrt{2}$ channels, and 6–8% for the $\sqrt{2}$ channels noted above, smaller in both cases than the likely 10% error induced by the same assumption for A_1 (the differential decay

rate is proportional to the square of the form factors)⁹. Systematic errors due to this approximation are within our statistical errors. A conservative estimate of the systematic error in the differential decay rate arising from this source can be obtained by adding in quadrature the 10% error due to A_1 and the worst-case 8% error from V and A_2 , to get a final error of 13%. We will see below that discretisation errors are expected to be almost twice as large as this.

We discussed in section 3 that we could not dismiss having 10% errors in the form factors arising from discretisation errors at the value of β used. In consequence, we will admit a 20% error in the decay rate which translates into a 10% error in $|V_{ub}|$. These errors are the largest among the systematic effects considered, and they almost entirely determine our overall systematic error. Combining errors from discretisation and our assumption of light quark spectator mass independence of the form factors in quadrature, we finally obtain an estimated 24% systematic error in the decay rate, which should be added to the results of table 4 and equations (26)–(28).

7 Conclusions

We have presented a method for extracting the CKM matrix element $|V_{ub}|$ from experimental measurements of the exclusive decay $\bar{B}^0 \rightarrow \rho^+ l^- \bar{\nu}_l$. We have shown how lattice simulations provide a model-independent framework in which nonperturbative QCD corrections can be systematically incorporated in the evaluation of the differential decay rate $d\Gamma(\bar{B}^0 \rightarrow \rho^+ l^- \bar{\nu}_l)/dq^2$ in a region of q^2 values from the charm threshold up to the zero recoil point, q_{max}^2 . We have measured points spanning roughly two-thirds of this region of q^2 . One of the main features of the approach presented here is that it does not rely upon large, difficult and model-dependent extrapolations in q^2 from q_{max}^2 down to values close to $q^2 = 0$, where the semileptonic decays are dominated by charmed final states, as in other previously suggested methods.

Discounting experimental errors, the results of table 4 will allow the determination of the CKM matrix element $|V_{ub}|$ with a theoretical uncertainty of less than 10% statistical and 12% systematic. Alternatively, determinations of $|V_{ub}|$ (with similar theoretical ambiguities) can be obtained from the overall normalisation of the hadronic effects parametrised by a , found to be

$$a = 4.6_{-0.3}^{+0.4} \text{ (stat)} \pm 0.6 \text{ (syst)} \text{ GeV}. \quad (29)$$

Both statistical and systematic theoretical errors will be reduced in forthcoming lattice simulations with smaller lattice spacing (to reduce discretisation errors, currently the principal systematic effect) and higher statistics.

⁹We have studied the effect on the results of the fit of equation (27) of having a 10% error in the $\sqrt{2}$ light meson momentum channels. This changes the parameter a by 5%.

Currently, only an upper bound for the total decay rate $\Gamma(\bar{B}^0 \rightarrow \rho^+ l^- \bar{\nu}_l)$ is known experimentally, but new results are forthcoming. It is important that the differential decay rate near q_{max}^2 be measured, since, as we have shown, such a measurement can provide a clean determination of $|V_{ub}|$ in the same way that similar measurements for the $\bar{B} \rightarrow D^*$ semileptonic decay have successfully been used to extract an accurate value for $|V_{cb}|$.

In this paper we have also determined the q^2 dependence of the form factor A_1 (which dominates the decay rate close to the zero recoil point) for the $\bar{B}^0 \rightarrow \rho^+ l^- \bar{\nu}_l$ decay in the region from $q^2 = 0$ to q_{max}^2 . The form factors V and A_2 , for the same semileptonic decay, have been studied in a region of q^2 around q_{max}^2 .

Finally, relations between radiative and semileptonic \bar{B} decays into light vector mesons, predicted by HQS, have been examined and found to hold within errors for the ratio $A_1/2iT_2$ and within 20% for the ratio $V/2T_1$ at the B scale.

Using extra momentum channels where the heavy-light meson is not at rest, but ω is nevertheless nearly constant as the heavy quark mass changes [36], has been essential for studying q^2 , or equivalently ω , dependences of A_1 , $A_1/2iT_2$, $V/2T_1$ and $d\Gamma/dq^2$. Knowledge of the q^2 dependence of $d\Gamma/dq^2$ has allowed us to determine the parameter a from a set of five measurements as well as from the zero recoil channel, giving us further confidence in our procedure for extracting $|V_{ub}|$.

Acknowledgements

We thank Chris Sachrajda and Hartmut Wittig for useful discussions. This research was supported by the UK Science and Engineering Research Council under grants GR/G 32779 and GR/H 49191, by the Particle Physics and Astronomy Research Council under grant GR/J 21347, by the University of Edinburgh and by Meiko Limited. We are grateful to Edinburgh University Computing Service and, in particular, to Mike Brown, for maintaining service on the Meiko i860 Computing Surface. DGR acknowledges the Particle Physics and Astronomy Research Council for support through an Advanced Fellowship. We acknowledge the Particle Physics and Astronomy Research Council for travel support under grant GR/J 98202.

References

- [1] See A J Buras and M K Harlander, in *Heavy Flavours*, Advanced Series on Directions in High Energy Physics — Vol 10, eds. A J Buras and M Lindner, World Scientific (1992) 58, and references therein
- [2] A Ali and D London, in Proc. XXVII Int. Conf. on High Energy Physics, Glasgow, eds. P J Bussey and I G Knowles, Institute of Physics Publishing (1994) 1133, and references therein

- [3] Particle Data Group, Phys. Rev. **D50** (1994) 1173
- [4] CLEO collaboration, J Bartelt *et al.*, Phys. Rev. Lett. **71** (1993) 4111
- [5] G Altarelli *et al.*, Nucl. Phys. **B208** (1982) 365
- [6] N Isgur *et al.*, Phys. Rev. **D39** (1989) 799; N Isgur and D Scora, Phys. Rev. **D40** (1989) 1491
- [7] M Wirbel, B Stech and M Bauer, Z. Phys. **C29** (1985) 637; M Bauer and M Wirbel, Z. Phys. **C42** (1989) 671
- [8] J G Körner and G A Schuler, Z. Phys. **C38** (1988) 511
- [9] C Ramirez, J F Donoghue and G Burdman, Phys. Rev. **D41** (1990) 1496
- [10] R J Morrison and J D Richman, Phys. Rev. **50** (1994) 1602
- [11] CLEO collaboration, A Bean *et al.*, Phys. Rev. Lett. **70** (1993) 2681
- [12] L K Gibbons, private communication
- [13] M Neubert, in Proc. XXVII Int. Conf. on High Energy Physics, Glasgow, eds. P J Bussey and I G Knowles, Institute of Physics Publishing (1994) 1129
- [14] M Shifman, in Proc. XXVII Int. Conf. on High Energy Physics, Glasgow, eds. P J Bussey and I G Knowles, Institute of Physics Publishing (1994) 1125
- [15] UKQCD collaboration, S P Booth *et al.*, Phys. Rev. Lett. **72** (1994) 462; UKQCD collaboration, K C Bowler *et al.*, Southampton preprint SHEP 95–06, Edinburgh preprint 95–525, Marseille preprint CPT–95–P–3179, hep-ph/9504231
- [16] L P Lellouch in Proc. LATTICE 94: 12th International Symposium on Lattice Field Theory, Bielefeld, Germany, Eds. F Karsch *et al.*, Nucl. Phys. B (Proc. Suppl.) **42** (1995) 421; Marseille preprint CPT–95/P.3196, to appear in Proc. XXX Rencontres de Moriond, Les Arcs, France, March 1995
- [17] CLEO collaboration, T E Browder, in Proc. XXVII Int. Conf. on High Energy Physics, Glasgow, eds. P J Bussey and I G Knowles, Institute of Physics Publishing (1994) 1117
- [18] ALEPH collaboration, I J Scott, in Proc. XXVII Int. Conf. on High Energy Physics, Glasgow, eds. P J Bussey and I G Knowles, Institute of Physics Publishing (1994) 1121

- [19] ARGUS collaboration, H Albrecht *et al.*, *Z. Phys.* **C57** (1993) 533
- [20] N Isgur and M B Wise, *Phys. Rev.* **D42** (1990) 2388
- [21] G Burdman and J F Donoghue, *Phys. Lett.* **B270** (1991) 55
- [22] P J O'Donnell and Q P Xu, *Phys. Lett.* **B325** (1994) 219; P J O'Donnell and H K K Tung, *Phys. Rev.* **D48** (1993) 2145
- [23] P Santorelli, *Z. Phys.* **C61** (1994) 449
- [24] P Colangelo, F De Fazio and P Santorelli, Bari preprint BARI-TH/94-174, hep-ph/9409438
- [25] B Grinstein, R Springer and M B Wise, *Nucl. Phys.* **B339** (1990) 269
- [26] M Neubert, *Phys. Rept.* **245** (1994) 259
- [27] P A Griffin, M Masip and M McGuigan, *Phys. Rev.* **D50** (1994) 5751
- [28] B Sheikholeslami and R Wohlert, *Nucl. Phys.* **B259**, 572 (1985).
- [29] G Heatlie *et al.*, *Nucl. Phys.* **B352**, 266 (1991).
- [30] UKQCD collaboration, C Allton *et al.*, *Phys. Rev.* **D49**, 474 (1994)
- [31] UKQCD collaboration, A K Ewing *et al.*, Southampton preprint SHEP-95-20
- [32] UKQCD collaboration, K C Bowler *et al.*, *Phys. Rev.* **D51** (1995) 4955
- [33] UKQCD collaboration, K C Bowler *et al.*, *Phys. Rev.* **D51** (1995) 4905
- [34] V Lubicz, G Martinelli, M S McCarthy and C T Sachrajda, *Phys. Lett.* **B274**, 415 (1992).
- [35] C Bernard, A El-Khadra and A Soni, *Phys. Rev.* **D43**, 2140 (1991); *Phys. Rev.* **D45**, 869 (1992).
- [36] UKQCD collaboration, D R Burford *et al.*, Southampton preprint SHEP-95-09, hep-lat/9503002, *Nucl. Phys. B* in press
- [37] A Borrelli *et al.*, *Nucl. Phys.* **B373** (1992) 781
- [38] G Martinelli, C T Sachrajda and A Vladikas, *Nucl. Phys.* **B358** (1991) 212
- [39] UKQCD collaboration, R M Baxter *et al.*, *Phys. Rev.* **D49** (1994) 1594
- [40] M E Luke, *Phys. Lett.* **B252** (1990) 447

- [41] A Ali, V M Braun and H Simma, *Z. Phys.* **C63** (1994) 437
- [42] A Abada *et al.*, *Nucl. Phys.* **B416** (1994) 675
- [43] APE collaboration, C R Allton *et al.*, *Phys. Lett.* **B345** (1995) 513
- [44] APE collaboration, A Abada *et al.*, Rome preprint ROME 94/1056, hep-lat/9503020
- [45] P Ball, V M Braun and H G Dosch, *Phys. Rev.* **D44** (1991) 3567; P Ball, *Phys. Rev.* **D48** (1993) 3190
- [46] S Narison, *Phys. Lett.* **B345** (1995) 166; *Phys. Lett.* **B283** (1992) 384
- [47] R N Faustov, V O Galkin and A Yu Mishurov, Cybernetics Council, Moscow, preprint, hep-ph/9505321
- [48] R Casalbuoni *et al.*, *Phys. Lett.* **B299** (1993) 139
- [49] B Stech, Heidelberg preprint HD-THEP-95-4, hep-ph/9502378